Melanopsin cells are the principal conduits for rod/cone input to non-image forming vision

Ali D. Güler[1,*], **Jennifer L. Ecker**[1,*], **Gurprit S. Lall**[2,*], **Shafiqul Haq**[3], **Cara M. Altimus**[1], **Hsi-Wen Liao**[3], **Alun R. Barnard**[2], **Hugh Cahill**[3], **Tudor C. Badea**[4], **Haiqing Zhao**[1], **Mark W. Hankins**[5], **David M. Berson**[6], **Robert J. Lucas**[2,†], **King-Wai Yau**[3], and **Samer Hattar**[1,†]

[1] Department of Biology, Johns Hopkins University, Baltimore, MD 21218, USA

[2] Faculty of Life Sciences, University of Manchester, Manchester M13 9PT, UK

[3] Department of Neuroscience, Johns Hopkins University-School of Medicine, Baltimore, MD 21205, USA

[4] Molecular Biology and Genetics, Johns Hopkins University-School of Medicine, Baltimore, MD 21205, USA

[5] Visual Neuroscience, University of Oxford, Oxford OX3 7BN, UK

[6] Department of Neuroscience, Brown University, Providence, RI 02912, USA

Abstract

Rod and cone photoreceptors detect light and relay this information through a multisynaptic pathway to the brain via retinal ganglion cells (RGCs)[1]. These retinal outputs support not only pattern vision, but also non-image forming (NIF) functions, which include circadian photoentrainment and pupillary light reflex (PLR). In mammals, NIF functions are mediated by rods, cones and the melanopsin-containing intrinsically photosensitive retinal ganglion cells (ipRGCs)[2, 3]. Rod/cone photoreceptors and ipRGCs are complementary in signalling light intensity for NIF functions[4–12]. The ipRGCs, in addition to being directly photosensitive, also receive synaptic input from rod/cone networks[13, 14]. To determine how the ipRGCs relay rod/cone light information for both image and non-image forming functions, we genetically ablated ipRGCs in mice. Here we show that animals lacking ipRGCs retain pattern vision, but have deficits in both PLR and circadian photoentrainment that are more extensive than those observed in melanopsin knockouts[8, 10, 11]. The defects in PLR and photoentrainment resemble those observed in animals that lack phototransduction in all three

photoreceptor classes[6]. These results indicate that light signals for irradiance detection are dissociated from pattern vision at the retinal ganglion cell level, and animals that cannot detect light for NIF functions are still capable of image formation.

The retinal ganglion cells that express melanopsin (rendering them intrinsically photosensitive) send monosynaptic projections to the suprachiasmatic nucleus (SCN) and the intergeniculate leaflet (IGL), responsible for circadian photoentrainment, and the olivary pretectal nucleus (OPN), responsible for PLR[15]. It has been reported that RGCs that do not contain melanopsin innervate the same NIF brain centres[15−19]. In mice genetically engineered to lack melanopsin protein, the RGCs that would normally express this opsin still project to the NIF centres, but these cells are no longer intrinsically photosensitive. In these animals, PLR and circadian light responses are reduced but not absent, indicating that rods/cones are capable of light detection for NIF functions[8−11]. The rod/cone signals for NIF functions are undoubtedly relayed to the brain by RGCs, but it is unclear whether ipRGCs, conventional RGCs, or both are responsible (Fig. 1a).

To eliminate ipRGCs, we introduced an attenuated diphtheria toxin A subunit ($aDTA$)[20] into the mouse melanopsin gene locus (Supplementary Fig. 1a, b). Using antibody staining in retinas from animals expressing $aDTA$ ($Opn4^{aDTA/+}$), we found 3.1±1.5% of melanopsin cells remained in the $Opn4^{aDTA/+}$ animals (Fig. 1b). X-gal staining in animals with the $aDTA$ gene in one melanopsin allele and $tau-LacZ$ in the other ($Opn4^{aDTA/tau-LacZ}$)[3] revealed that 17.2 ±1.0% of melanopsin cells remained in the retinas of these animals at 6 months of age (Fig. 1c). Consistent with the elimination of ipRGCs, we observed fewer fibre terminals in the SCN, IGL and OPN of $Opn4^{aDTA/tau-LacZ}$ compared to $Opn4^{tau-LacZ/+}$ animals (Fig. 2a–c). The degree of ipRGC ablation in the heterozygous animals increased with age (Supplementary Fig. 2a–c).

To more completely ablate ipRGCs, we generated animals homozygous for $aDTA$ ($Opn4^{aDTA/aDTA}$). The morphology and thickness of the retina in the $Opn4^{aDTA/aDTA}$ animals was not different from wild types (Fig. 1d). Injection of fluorescently conjugated cholera toxin in the eye, which labels all ganglion cell fibres from the retina, showed that few fibres innervated the SCN and IGL in the $Opn4^{aDTA/aDTA}$ animals (Fig. 2d, e). Furthermore, comparison between age-matched $Opn4^{aDTA/+}$ and $Opn4^{aDTA/aDTA}$ mice verified that the extent of ipRGC ablation was greater in homozygous animals (Supplementary Fig. 2d). We also observed that target innervation by other RGCs was unaffected both in the dorsal lateral geniculate nucleus, which is important for image formation, and in the rostral core of the OPN[15] (Fig. 2e, f).

To assess whether image-forming functions are affected in animals expressing aDTA, we measured electroretinograms, optokinetic nystagmus responses (OKN), visual acuity and the ability of the animals to detect a visual cue. We found that the electroretinograms and OKN were normal in animals that lack ipRGCs (Supplementary Fig. 3a, b). Based on optomotor responses, the acuity of $Opn4^{aDTA/aDTA}$ mice was slightly decreased compared to wild-type (Fig. 1e) and $Opn4^{tau-LacZ/tau-LacZ}$ mice (Supplementary Fig. 3d). This effect is most likely due to enlarged pupil diameters in the $Opn4^{aDTA/aDTA}$ animals (see Fig. 3c and Supplementary Fig. 3c). We also determined that these animals could use a visual cue to locate a flag-marked platform in a water maze paradigm (Fig. 1e). These results demonstrate that image formation is functional despite the elimination of ipRGCs in $Opn4^{aDTA/aDTA}$ animals. Therefore, we could determine the relative contribution of ipRGCs to PLR and circadian photoentrainment in the context of normal image formation.

Pupil constriction regulates the amount of light entering the eye and thus pupil diameter is negatively correlated with light intensity. At high light intensity, the iris decreases the area of

the pupil by 95% (full constriction) compared to dark-adapted conditions (fully dilated). At low light intensity in which the pupil constricts 50% or less, rod/cone input is the main signal[8, 12] (Supplementary Table 1). On the other hand, the intrinsic photosensitivity through the melanopsin protein in ipRGCs is necessary for full pupil constriction[8, 12] (Supplementary Table 1). We found that the PLR was absent in all $Opn4^{aDTA/+}$ mice at a light intensity that constricts the pupil in wild-type animals to ~50% (Fig. 3a, b). This result suggests that although the melanopsin protein is not required for PLR at low light intensity, rod/cone input still requires the ipRGCs. We propose that ipRGCs are able to code light intensities that are below the detection level of the melanopsin photopigment by integrating rod/cone signals and relaying this information to the OPN for pupil constriction.

At high light intensity, 6 of 9 $Opn4^{aDTA/+}$ mice constricted their pupils to 95%, similar to wild-type animals (Fig. 3a, b). Full pupil constriction in these 6 animals indicates that the intrinsic photosensitivity persists in the remaining ipRGCs in $Opn4^{aDTA/+}$ mice and that only ~17% of ipRGCs are sufficient to drive full pupil constriction. The remaining 3 animals had pupil constriction defects at high light intensity (59±14% compared to 96±1% in wild type; Fig. 3b). Interestingly, when the $Opn4^{aDTA/+}$ animals were placed under 24-hour light/dark cycles, animals that had full pupil constriction photoentrained (Supplementary Fig. 4a), while animals with defective pupil constriction had photoentrainment defects (Supplementary Fig. 4b).

The $aDTA$ homozygotes have greater ablation of ipRGCs, and consequently all 12 $Opn4^{aDTA/aDTA}$ animals had defective PLR (42±6%) at high light intensity (Fig. 3c, d). It is noteworthy to mention that similar pupil constriction (~40%) to that observed in $Opn4^{aDTA/aDTA}$ mice is achieved by both wild-type and melanopsin knockout animals to a light stimulation that is ~1000-fold less in intensity[8]. This reduction in pupil sensitivity was observed in an intensity response curve in $Opn4^{aDTA/aDTA}$ mice at constrictions that are 55% or higher in the wild types (Supplementary Fig. 5). Together, these data show that the rod/cone-dependent pupil constriction is reliant on signalling through ipRGCs at all light intensities (Fig. 3 and Supplementary Fig. 5). The residual pupil constriction observed in the homozygous animals may reveal a possible role for the non-melanopsin RGCs in pupil constriction. Alternatively, this residual pupil constriction could originate from rod/cone input through a few remaining ipRGCs in the $Opn4^{aDTA/aDTA}$ mice.

To assess the contribution of ipRGCs to circadian photoentrainment, we analyzed the wheel-running activity of wild-type (n=11) and $Opn4^{aDTA/aDTA}$ (n=12) animals using 24-hour light dark cycles. Under constant dark conditions (DD) both wild-type and $Opn4^{aDTA/aDTA}$ animals had a functional circadian oscillator with period lengths of 23.3±0.1 and 23.8±0.1, respectively (Fig. 4a). Similar to Math5$^{-/-}$ mice with severe optic nerve hypoplasia, $Opn4^{aDTA/aDTA}$ animals had significantly longer periods compared to wild types (Supplementary Table 2) confirming the loss of the fibres projecting to the SCN[21]. A light stimulus (1500 lux) administered for 15 minutes at CT16 delayed the phase onset of the activity of the wild types by 1.66±0.23 hours while it did not affect the phase onset of activity in any $Opn4^{aDTA/aDTA}$ animals (−0.06±0.09 hours) (Fig. 4a). When the light/dark cycle was advanced or delayed by 6 hours, the activity of all wild-type animals synchronized with the shifted cycle (Fig. 4b and Supplementary Table 2). $Opn4^{aDTA/aDTA}$ animals segregated into two groups with distinct responses. The first group of animals (8 of 12) free ran completely under the shifted light/dark cycle (Fig. 4b and Supplementary Fig. 6b–f) similar to animals that lack all functional photoreceptors in the retina[6], indicating that they were completely blind to the light shift. The second group of animals (4 of 12) was weakly light responsive, but not photoentrained, since they did not display a stable phase relation to the light/dark cycle (Supplementary Fig. 7). Given that these 4 animals demonstrated very weak light responsiveness in the light/dark cycle, but were not phase-shifted by the 15 minute light pulse, we tested whether constant light (LL) conditions would lengthen the circadian period of $Opn4^{aDTA/aDTA}$ mice. Under LL, 7 of 11 wild-type animals had periods

longer than 24 hours[10], while the other 4 animals became completely arrhythmic (Supplementary Fig. 6a). In contrast, both groups of *Opn4^aDTA/aDTA* animals had periods shorter than 24 hours (Fig. 4c, Supplementary Fig. 6b–f, 7 and Supplementary Table 2). Previously, it had been demonstrated that animals lacking only the melanopsin protein are similar to wild-type controls in adjusting to a 24-hour light/dark cycle and have only minor defects in both their period lengthening under constant light and phase-delaying pulses of light[10, 11]. The severe defects in circadian photoentrainment observed in animals lacking ipRGCs demonstrate that these cells are required not only for intrinsically signalling light information through the melanopsin protein, but also for conveying rod/cone light information to the SCN. Although several reports indicated that RGCs that do not express melanopsin innervate the SCN[17–19, 22], our results reveal that the contribution of rod/cone signalling through these RGCs for photoentrainment is negligible.

The acute effects of light on activity (also known as masking) can be studied by utilizing an ultradian 7-hour light/dark (3.5:3.5 LD) cycle that disrupts the oscillator[6]. Under the ultradian paradigm, wild types confined their activity mostly to the dark portion of the ultradian cycle (84±4%). In contrast, the *Opn4^aDTA/aDTA* animals were active nearly randomly across an ultradian day irrespective of light (64±3%; Fig. 4d). This result demonstrates that melanopsin-containing cells are essential for a direct light-driven physiological response that is independent of the circadian oscillator.

In summary, we have shown that the loss of ipRGCs does not influence image formation and therefore involvement of this ganglion cell class in classical vision is only modulatory[13, 23]. In contrast, irradiance-dependent NIF functions are substantially impaired in the absence of ipRGCs. Given that the ipRGCs constitute less than 2% of the total RGC population, it is striking that light information for circadian photoentrainment and PLR is predominantly conveyed through these cells. Moreover, the ability to form pattern vision does not impact photoentrainment.

Methods Summary

Animals

All experiments were conducted in accordance with NIH guidelines and approved institutional animal care and use committees of the Universities involved.

Behavioural analyses

We used behavioural tests that measure the integrity of the outer retina (electroretinograms) [23], eye tracking functions (optokinetic nystagmus)[24], visual acuity (optomotor)[25], object identification (water maze)[26], pupil constriction (PLR)[8, 12], the period of the circadian oscillator (wheel running activity)[10, 11], the adjustment of the circadian clock to different light stimulations (circadian photoentrainment, phase shifting, and constant light) [10, 11] and direct light effects on activity (masking)[9].

Methods

aDTA mice

Using the homologous arms that we used previously[3], we targeted the *aDTA* gene to the melanopsin locus. The targeting construct contained the diphtheria toxin A subunit and the neomycin resistance genes. The construct was flanked by a 4.4kb 5′ of the ATG site of the mouse melanopsin gene, and a 1.6kb fragment containing 654bp of exon9 plus 946bp 3′UTR. Following electroporation of the linearized construct into 129.1 mouse strain embryonic stem (ES) cells and drug selection (400μg/ml of G418), one positive ES clone was injected into

C57BL/6 blastocysts. Chimeric animals were mated to C57BL/6 mice to produce heterozygous animals.

Immunostaining

Whole retinas from *Opn4*$^{aDTA/+}$ and wild-type animals, fixed in 70% ethanol, were immunostained using the c-terminus melanopsin antibody (1:500 dilution). Fluorescently-conjugated secondary antibody (Alexa Fluor 488 goat anti-rabbit IgG (1:1000 dilution), Molecular Probes, OR) was applied for 1–3hrs.

X-gal staining

Animals anaesthetized by intraperitoneal injection of Avertin (20ml/kg) were intracardially perfused with 4% paraformaldehyde, and brains and eyes isolated. Eye-cups or brain sections (50micron) were first incubated in Buffer B (100mM phosphate buffer at pH7.4, 2mM $MgCl_2$, 0.01% sodium deoxycholate, 0.02% IGEPAL) then stained in Buffer B plus 5mM potassium ferricyanide, 5mM potassium ferrocyanide, and 1mg/ml X-gal for 3 days.

Cholera toxin injections in the eye

Mice were anesthetized with Ketamine (80mg/kg)/Xylazine (8mg/kg). Eyes were injected intravitreally with 2μL of cholera toxin B subunit conjugated with Alexa Fluor 488 or 555 (Invitrogen, CA). Three days after injection, brains were isolated and sectioned.

Electroretinograms

Animals maintained under 12:12 light/dark cycles for 3 days were used to collect data within the light phase (after 50mins dark adaptation). The ERG setup was similar to that we used previously[23]. Mydriatics (tropicamide 1% and phenylephrine 2.5%) and hypromellose solution (0.3%) were used to dilate the pupil and retain corneal moisture in anesthetized mice. A signal conditioner (Model 1902 Mark III, Cambridge Electronic Design, Ltd., CED, UK) differentially amplified (×3000) and filtered (band-pass filter cut-off 0.5 to 200Hz) the signal before it was digitized (Model 1401, CED) and recorded (sampling rate 10kHz) via the Signal 2.15 Software (CED, UK).

White light (10ms in duration) was provided by a xenon arc source (Cairn Research, Ltd., UK). Neutral density filters (Edmund Optics, UK) were used (unattenuated intensity, 320 μW/cm^2 at the cornea). For scotopic recordings, flashes were administered in the dark and testing began with the dimmest stimulus. Depending on the intensity, stimuli were presented at a rate of 0.5 to 0.2Hz and 6–20 repetitions were collected and averaged. Photopic ERGs were recorded by presentation of an unattenuated light (20 stimuli presented at a rate of 1Hz) against blue filtered (Grass blue filter, Astro-Med, RI) rod-saturating background light (160μW/cm^2).

OKN

A mouse stabilized with a head post was placed into an acrylic holder in a 12′ inch diameter drum. Computer generated stimuli were projected down onto the drum walls. Black and white stripes 4 degrees in width were rotated at five degrees per second. Mice eye movements were captured with an infrared video system. The fast saccade components were counted per 30-second intervals using an algorithm, which evaluated the high velocity eye movements that followed a slow velocity movement in the opposite direction (ISCAN, MA).

Visual Acuity

A virtual cylinder "OptoMotry" (Cerebral Mechanics, Lethbridge, Canada) was used to determine visual acuity by measuring the image-tracking reflex of mice[25]. A sine wave grating was projected on the screen rotating in a virtual cylinder. The animal was assessed for a tracking

response upon stimulation for approximately 5 seconds. All acuity thresholds were determined using the staircase method with 100% contrast.

Morris Water Maze

In order to assess the ability of mice to detect a visual cue, we trained the animals to find a platform marked by a 10cm tall, high contrast visual cue under bright light (500lux) in an 85cm pool. On day one, mice were trained with 4 trials 15 minutes apart. On the following day, latency to find the island was recorded first with and second without the cue.

PLR

All animals were dark adapted for at least one hour and the eye of each animal receiving the photic stimulus was treated with 0.1% atropine prior to the start of recording. Measurements were restricted to the middle of the subjective day (CT 4–8). One eye of each mouse was digitally captured at a frequency of 1 image per second for 63 seconds using a CCD camera. The light stimuli (xenon arc light source) consisted of a 60 second pulse at an intensity of 3.8mW/cm^2 or 1.8μW/cm^2 of white light. For the $Opn4^{aDTA/aDTA}$ experiments, the eye receiving the photic stimulus was treated with 1% atropine. While one eye received light stimulation from a 470nm LED light source (E27-B24, Super Bright LEDs, MO; 161μW/cm^2), a digital camcorder (Sony DCRHC96, Japan) was used to record from the other eye (30 seconds) at 30frames/second under a 940nm light (LDP LLC, NJ). The digital video recoding was deconstructed to individual frames using Blaze MediaPro Software (Mystik Media, NC). The percent pupil constriction was calculated as the percent of pupil area at 30 seconds after the initiation of the stimulus (steady state) relative to the dilated pupil size.

Wheel Running Activity

Mice were placed in cages with a 4.5-inch running wheel and their activity was monitored with VitalView software (Mini Mitter, OR). Period was calculated using ClockLab (Actimetrics, IL). For phase shifting experiments, each animal was exposed to a light pulse (1500lux; CT16) for 15min. After 41 days of constant dark, mice were then re-entrained to 12:12 light/dark cycles for 19 days. Animals were then exposed to two jet-lag paradigms: 16 days of a six-hour advance followed by 32 days of a six-hour delay. During the last two weeks of this treatment the animals were tested for PLR. Animals were then exposed to constant light for three weeks followed by an ultradian 3.5:3.5 light/dark cycles.

Supplementary Material

Refer to Web version on PubMed Central for supplementary material.

Acknowledgments

References

1. Hubel, DH. Eye, brain, and vision (Scientific American Library). W.H. Freeman; New York: 1988.
2. Berson DM, Dunn FA, Takao M. Phototransduction by retinal ganglion cells that set the circadian clock. Science 2002;295:1070–3. [PubMed: 11834835]

3. Hattar S, Liao HW, Takao M, Berson DM, Yau KW. Melanopsin-containing retinal ganglion cells: architecture, projections, and intrinsic photosensitivity. Science 2002;295:1065–70. [PubMed: 11834834]

4. Freedman MS, et al. Regulation of mammalian circadian behavior by non-rod, non-cone, ocular photoreceptors. Science 1999;284:502–4. [PubMed: 10205061]

5. Czeisler CA, et al. Suppression of melatonin secretion in some blind patients by exposure to bright light. N Engl J Med 1995;332:6–11. [PubMed: 7990870]

6. Hattar S, et al. Melanopsin and rod-cone photoreceptive systems account for all major accessory visual functions in mice. Nature 2003;424:75–81.

7. Panda S, et al. Melanopsin is required for non-image-forming photic responses in blind mice. Science 2003;301:525–7. [PubMed: 12829787]

8. Lucas RJ, et al. Diminished pupillary light reflex at high irradiances in melanopsin-knockout mice. Science 2003;299:245–7. [PubMed: 12522249]

9. Mrosovsky N, Hattar S. Impaired masking responses to light in melanopsin-knockout mice. Chronobiol Int 2003;20:989–99. [PubMed: 14680139]

10. Panda S, et al. Melanopsin (*Opn4*) requirement for normal light-induced circadian phase shifting. Science 2002;298:2213–6. [PubMed: 12481141]

11. Ruby NF, et al. Role of melanopsin in circadian responses to light. Science 2002;298:2211–3. [PubMed: 12481140]

12. Lucas RJ, Douglas RH, Foster RG. Characterization of an ocular photopigment capable of driving pupillary constriction in mice. Nat Neurosci 2001;4:621–6. [PubMed: 11369943]

13. Dacey DM, et al. Melanopsin-expressing ganglion cells in primate retina signal colour and irradiance and project to the LGN. Nature 2005;433:749–54. [PubMed: 15716953]

14. Wong KY, Dunn FA, Graham DM, Berson DM. Synaptic influences on rat ganglion-cell photoreceptors. J Physiol. 2007

15. Hattar S, et al. Central projections of melanopsin-expressing retinal ganglion cells in the mouse. J Comp Neurol 2006;497:326–49. [PubMed: 16736474]

16. Gooley JJ, Lu J, Fischer D, Saper CB. A broad role for melanopsin in nonvisual photoreception. J Neurosci 2003;23:7093–106. [PubMed: 12904470]

17. Hannibal J, Fahrenkrug J. Target areas innervated by PACAP-immunoreactive retinal ganglion cells. Cell Tissue Res 2004;316:99–113. [PubMed: 14991397]

18. Morin LP, Blanchard JH, Provencio I. Retinal ganglion cell projections to the hamster suprachiasmatic nucleus, intergeniculate leaflet, and visual midbrain: bifurcation and melanopsin immunoreactivity. J Comp Neurol 2003;465:401–16. [PubMed: 12966564]

19. Sollars PJ, et al. Melanopsin and non-melanopsin expressing retinal ganglion cells innervate the hypothalamic suprachiasmatic nucleus. Vis Neurosci 2003;20:601–10. [PubMed: 15088713]

20. Maxwell F, Maxwell IH, Glode LM. Cloning, sequence determination, and expression in transfected cells of the coding sequence for the tox 176 attenuated diphtheria toxin A chain. Mol Cell Biol 1987;7:1576–9. [PubMed: 3110596]

21. Wee R, Castrucci AM, Provencio I, Gan L, Van Gelder RN. Loss of photic entrainment and altered free-running circadian rhythms in *math5−/−* mice. J Neurosci 2002;22:10427–33. [PubMed: 12451142]

22. Gooley JJ, Lu J, Chou TC, Scammell TE, Saper CB. Melanopsin in cells of origin of the retinohypothalamic tract. Nat Neurosci 2001;4:1165. [PubMed: 11713469]

23. Barnard AR, Hattar S, Hankins MW, Lucas RJ. Melanopsin regulates visual processing in the mouse retina. Curr Biol 2006;16:389–95. [PubMed: 16488873]

24. Iwakabe H, Katsuura G, Ishibashi C, Nakanishi S. Impairment of papillary responses and optokinetic nystagmus in the mGluR6-deficient mouse. Neuropharmacology 1997;36:135–43. [PubMed: 9144650]

25. Prusky GT, Alam NM, Beekman S, Douglas RM. Rapid quantification of adult and developing mouse spatial vision using a virtual optomotor system. Invest Ophthalmol Vis Sci 2004;45:4611–6. [PubMed: 15557474]

26. Vorhees CV, Williams MT. Morris water maze: procedures for assessing spatial and related forms of learning and memory. Nat Protoc 2006;1:848–58. [PubMed: 17406317]
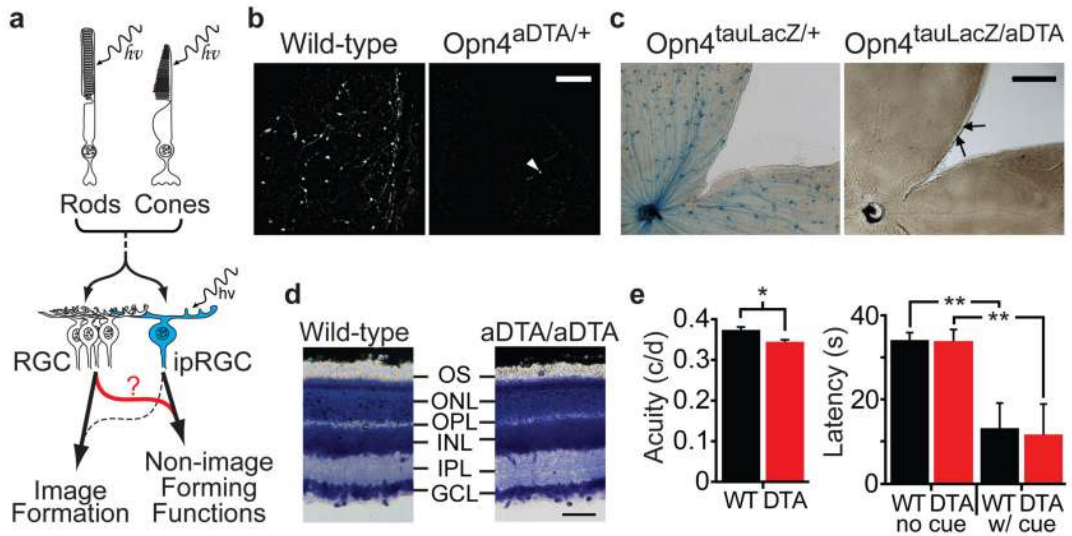
Figure 1. Elimination of ipRGCs in mouse retina
a, Model describing how rod/cone signalling through conventional RGCs or ipRGCs contribute to NIF functions. Role of ipRGCs in image formation is speculative (dotted line). **b,** Melanopsin antibody staining in retinas of 18 month old wild-type (n=6) and *Opn4^aDTA/+* (n=12) mice. White arrowhead indicates a surviving ipRGC. Scale bar, 200μm. **c,** X-gal staining from *Opn4^tau-LacZ/+* (n=6) and *Opn4^aDTA/tau-LacZ* (n=8). The surviving cells are weakly stained (black arrows). Scale bar, 500μm. **d,** Cross sections of Giemsa stained retinas from 18 month old *Opn4^aDTA/aDTA* (aDTA/aDTA; n=3) and wild-type mice (n=3). The morphology of retinas is indistinguishable between genotypes. GCL, ganglion cell layer; IPL, inner plexiform layer; INL, inner nuclear layer; OPL, outer plexiform layer; ONL, outer nuclear layer; OS, outer segment. Scale bar, 50 μm. **e,** Left, the acuity of *Opn4^aDTA/aDTA* mice (DTA; n=11; red bar) was slightly decreased compared to wild types (WT; n=9; black bar). Right, the latency to locate a marked platform (w/cue) in a water maze was similar between *Opn4^aDTA/aDTA* (DTA; n=14; red bar) and wild types (WT; n=12; black bar). This latency significantly differed for unmarked platform (no cue) tests. All statistical comparisons utilized Student's *t* test (*, $p<0.05$; **, $p<0.01$); error bars ± s.e.m.
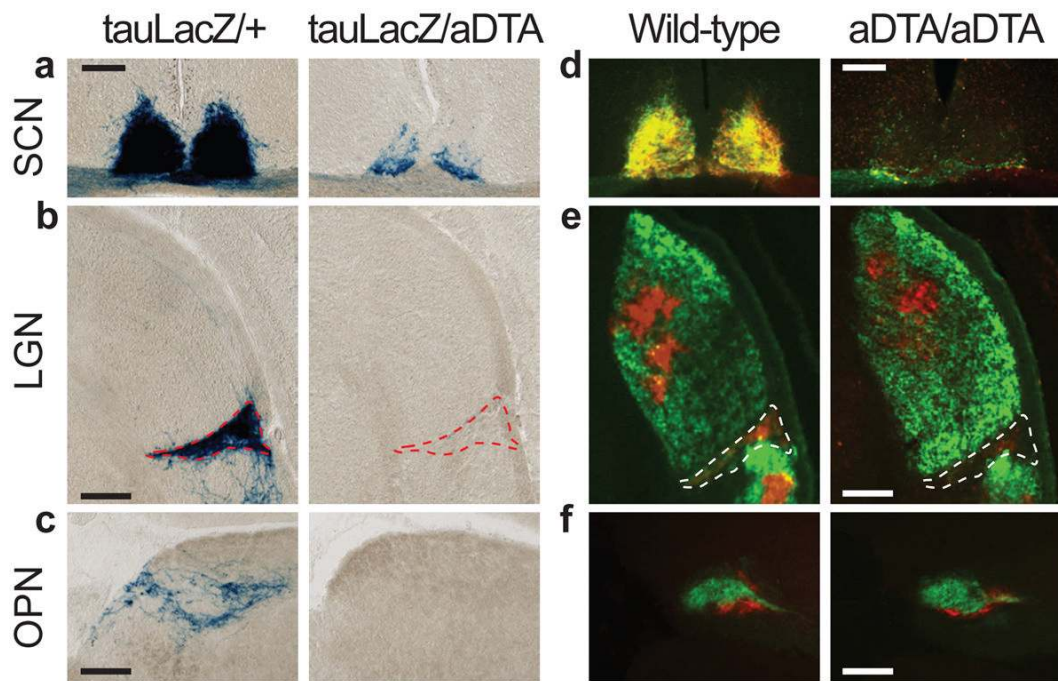
Figure 2. The ipRGC fibres in the brain decrease in *aDTA* mice
a, b, and c, X-gal staining in $Opn4^{tau-LacZ/aDTA}$ (tauLacZ/aDTA; n=2) show that ipRGC innervation of the SCN, IGL and OPN is decreased. **d, e, and f**, Ocular cholera toxin injections (left eye, green; right, red) of $Opn4^{aDTA/aDTA}$ (aDTA/aDTA; n=11) and wild types (n=6). **a and d,** SCN innervation is sparse in *aDTA* mice. **b and e,** The dorsal lateral geniculate nucleus (LGN) is innervated similarly both in *aDTA* and wild-type animals, while few fibres remain in the IGL of mutant mice (outlined region). **c and f,** The OPN shell is innervated by ipRGCs and the core is targeted by other RGCs[15]. **f,** Fibres in the OPN core are retained in $Opn4^{aDTA/aDTA}$ mice. **c,** Fibres in the shell region are eliminated in $Opn4^{tau-LacZ/aDTA}$ animals. Scale bars, 200μm.
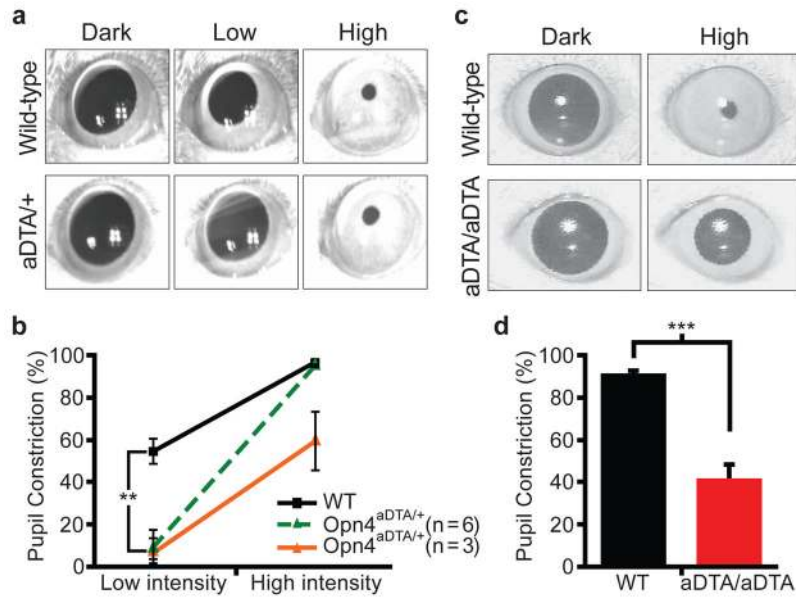
Figure 3. *Opn4^aDTA* mice have deficits in PLR
a, All 9 *Opn4^aDTA/+* mice showed defective PLR ($1.8\mu W/cm^2$; 30s white light; Low) that induces 50% constriction in wild types. The *Opn4^aDTA/+* mice showed a 9.0±6.0% constriction. 6 of 9 *Opn4^aDTA/+* mice had full pupil constriction at high light intensity ($3mW/cm^2$; High). The rest of the mutant mice (3 of 9) showed defective PLR. **b**, Quantification of PLR data of wild-type (WT; n=9; black squares) and *Opn4^aDTA/+* either photoentrained (green triangles; n=6) or non-photoentrained (orange triangles; n=3) animals. All statistical comparisons were made by Student's *t* test (**, *p*<0.01). **c,** All *Opn4^aDTA/aDTA* animals constrict their pupil only to a maximum of 42% at a light pulse that causes 95% constriction in wild types ($161\mu W/cm^2$, 470nm monochromatic light; High). **d,** Quantification of PLR data of wild-type (WT; n=11; black bar) and *Opn4^aDTA/aDTA* (aDTA/aDTA; n=12; red bar) mice from c. Statistical comparisons were made by Student's *t* test (***, *p*<0.001); error bars ± s.e.m.

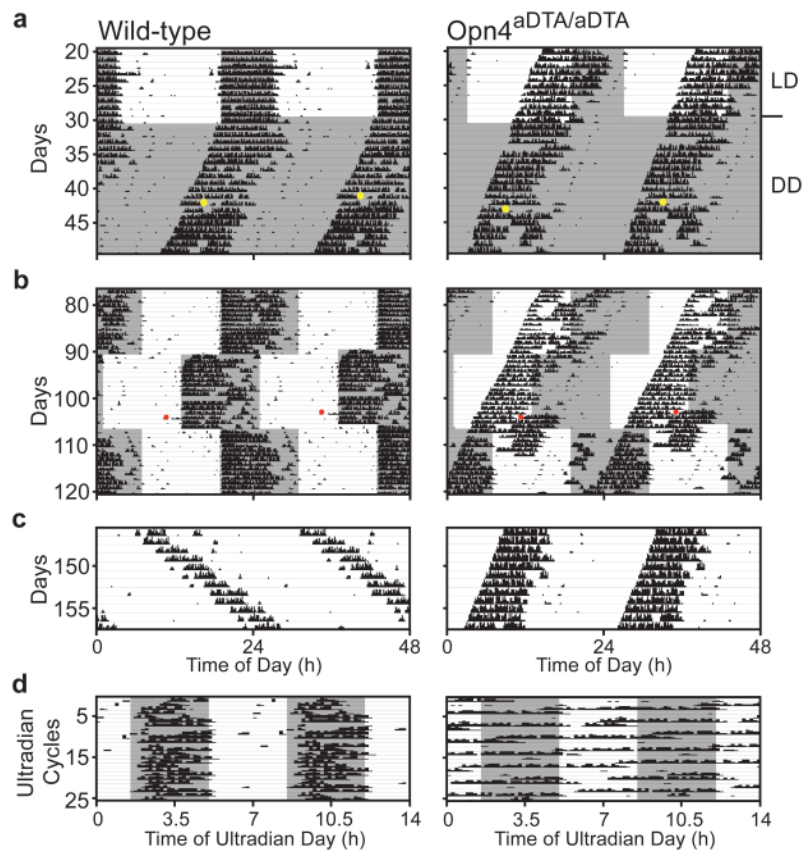**Figure 4.** *Opn4^aDTA/aDTA* **mice do not photoentrain or mask**
a, *Opn4^aDTA/aDTA* mice free-run under light/dark cycles (grey and white backgrounds; dark and light (~700lux), respectively). *Opn4^aDTA/aDTA* mice do not phase shift to a 15-minute 1500lux white light pulse (CT16; yellow dots: light pulses). **b,** *Opn4^aDTA/aDTA* mice do not photoentrain to the 24-hour light/dark cycle in the delay or advance phases. **c,** Unlike wild-type animals, no *Opn4^aDTA/aDTA* mice lengthened their period under constant light. **d,** *Opn4^aDTA/aDTA* mice do not mask under 7-hour ultradian cycle. Red dots: cage changes.